

A Continuum of Optimal Tetrahelices between the Boerdijk-Coxeter Helix and a Planar-faced Tetrahelix

Robert L. Read

Founder, Public Invention
Austin, TX, 78704

Email: read.robert@gmail.com

The Boerdijk-Coxeter helix (BC helix, or tetrahelix) is a face-to-face stack of regular tetrahedra forming a helical column. Treating the edges of these tetrahedra as structural members creates an attractive and inherently rigid space frame, and therefore interesting to architects, mechanical engineers, and roboticists. A formula is developed that matches the visually apparent helices forming the outer rails of the BC helix. This formula is generalized to a formula convenient to designers. Formulae for computing the parameters that give proven edge-length minimax-optimal tetrahelices are given, defining a continuum of optimum tetrahelices of varying curvature. The endpoints of this continuum are the BC helix and a structure of zero curvature, the *equitetrabeam*. Only one out of three members in the system change their length to reach any point in the continuum. Numerically finding the rail angle from the equation for pitch allows optimal tetrahelices of any pitch to be designed. An interactive tool for such design and experimentation is provided: <https://pubinv.github.io/tetrahelix/>. A formula for the inradius of optimal tetrahelices is given. The continuum allows a regular Tetrobot supporting a length change of less than 16% in the BC configuration to untwist into a hexapodal or n -podal robot to use standard gaits.

1 Introduction

The Boerdijk-Coxeter helix [1] (BC helix) (see figs. 1 and 2), is a face-to-face stack of tetrahedra that winds about a straight axis. Architects, structural engineers, and roboticists are inspired by and follow such regular mathematical models. However, since they can also build structures and machines from members of differing or even dynamically changing length, it is useful to develop the mathematics of structures formed from tetrahedra where we relax regularity.

The vertices of the tetrahedra lie upon three helices about the central axis. The Tetrobot [2, 3] uses the regularity of this geometry to make a tentacle-like robot that can crawl like a slug or mollusk. These modular robotic systems use mechanical actuators which can change their length, connected by special joints, such as the 3D printable

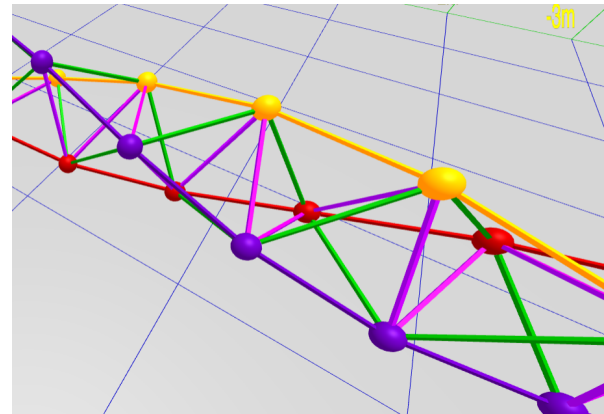


Fig. 1. BC Helix Close-up (partly along axis)

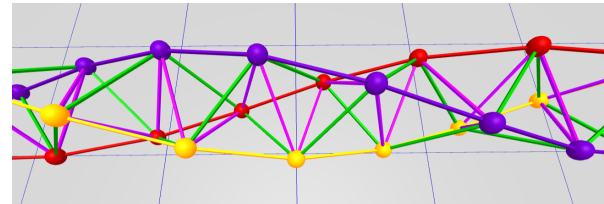


Fig. 2. BC Helix Close-up (orthogonal)

Song-Kwon-Kim [4] joint or the CMS joint [5] used in the original Tetrobot. This allows many members to meet in a single point. Such machines can follow purely regular mathematical models such as the Boerdijk-Coxeter helix or the Octet Truss [6].

Buckminster Fuller called the BC helix a *tetrahelix* [7], a term now commonly used. In this paper, we reserve *BC helix* to mean the purely regular structure and use *tetrahelix* to refer to any structure isomorphic to the BC helix.

Imagining fig. 1 or fig. 2 as a static mechanical structure, we can observe that it is useful to the mechanical engineer because the structure is a mechanically strong, inherently rigid, omni-triangulated space frame. Then we can imagine that each static edge is replaced with an actuator that can dy-

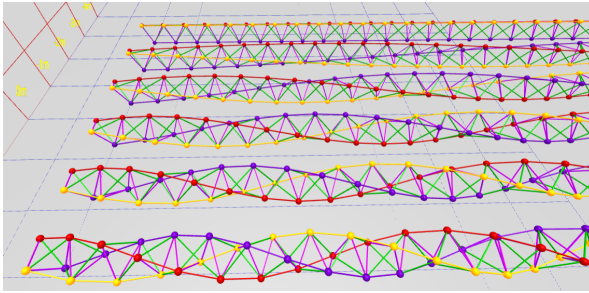


Fig. 3. A Continuum of Tetrahelices

namically become shorter or longer in response to electronic control, and the vertices are joints that support sufficient angular displacement for this to be possible. An example of such a machine is a Tetrobot, shown in fig. 5.

A BC helix does not rest stably on a plane. It is convenient to be able to “untwist” it and to form a tetrahelix space frame that has a flat planar surface. By making length changes in a certain way, we can untwist a tetrahelix to form a *tetrabeam* which has planar faces and has, for example, an equilateral triangular profile. This paper develops the equations needed to untwist the tetrahelix. All math developed here is available in JavaScript and demonstrated by an interactive design website <https://pubinv.github.io/tetrahelix/> [8], from which figs. 1 and 2 and later figures in this paper are taken.

Figure 3 displays a continuum of tetrahelices optimal in a certain sense, which is the main result of this paper. The closest helix is the BC helix, and the furthest is the equitetrabeam, defined in section 6 and figs. 9 and 10.

Trusses and space frames remain an important design field in mechanical and structural engineering [9], including deployable and moving trusses [10, 11].

1.1 Utility for Robotics

Starting twenty years ago, Sanderson [12], Hamlin, [3], Lee [13], and others created a style of robotics based on changing the lengths of members joined at the center of a joint, thereby creating a connection to pure geometry. More recently, NASA has experimented with tensegrities [14, 15], a different point in the same design spectrum. In particular, the tetrahelix is related to the tetraspline [16] concept used as a model of a tensegrity robot. Although tensegrities are not member-for-member isomorphic to the tetrahelix as the tetrobot is, they often use repeated tetrahedral cells, so this work of pure geometry has some applied relevance to them.

As suggested by Buckminster Fuller, the most convenient geometries to consider are those that have regular member lengths, in order to facilitate the inexpensive manufacture and construction of the robot. In a plane, the octet truss [6] is such a geometry, but in a line, the Boerdijk-Coxeter helix is such a regular structure.

However, a robot must move, and so it is interesting to consider the transmutations of these regular geometries. Developing a functional gait for our physical Tetrobot (the 7-Tet Glussbot) was in fact the motivation for this work. By

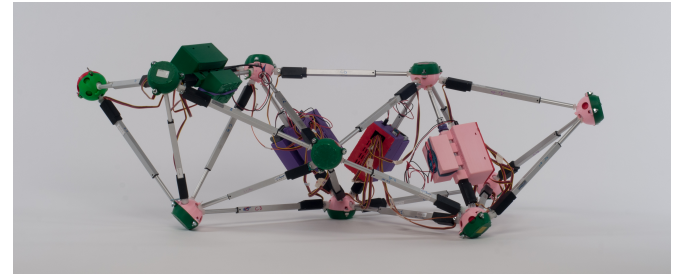


Fig. 4. 7-Tet Tetrobot in relaxed, or BC helix configuration

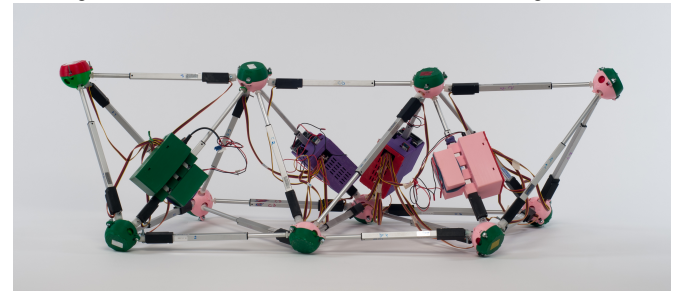


Fig. 5. The Equitetrabeam: Fully Untwisted 7-Tet Tetrobot in Hexapod Configuration

changing only the length of only one third of the members, we can dynamically untwist a physical Tetrobot forming the Boerdijk-Coxeter configuration into the equitetrabeam which rests flat on the plane, as shown in fig. 5.

By untwisting the tetrahelix so that it has a planar surface resting on the ground, we may consider each vertex touching the ground a foot or pseudopod. A robot can thus become a hexapod or n -pod Tetrobot, and the already well-developed approaches to hexapod gaits may be applied to make the robot walk or crawl.

2 A Designer’s Formulation of the BC Helix

We would like to design nearly regular tetrahelices with a formula that gives the vertices in space. Eventually, we would like to design them by choosing the lengths of a small set of members. In a space frame, this is a static design choice; in a Tetrobot, it is a dynamic choice that can be used to twist the robot and/or exert linear or angular force on the environment.

Ideally, we would have a simple formula for defining the vertices based on any curvature or pitch we choose. It is a goal of this paper to relate the Cartesian coordinate approach and the member-length approach to generating a tetrahelix continuum.

H.S.M Coxeter constructs the BC helix [1] as a repeated rotation and translation of the tetrahedra by showing the rotation is:

$$\theta_{bc} = \arccos(-2/3) \quad (1)$$

and the translation:

$$h_{bc} = 1/\sqrt{10}. \quad (2)$$

Note that θ_{bc} is approximately $0.37 \cdot 2\pi$ radians or 131.81 degrees. The angle θ_{bc} is the rotation of *each* tetrahedron, not the tetrahedra along a rail. In fig. 1, each tetrahedron has either a yellow, blue, or red outer edge or rail. That is, a blue-rail tetrahedron is rotated slightly more than a $1/3$ of a revolution to match the face of the yellow tetrahedron.

R.W. Gray's website [17], repeating a formula by Coxeter [1] in a more accessible form, gives the Cartesian coordinates $\begin{bmatrix} x \\ y \\ z \end{bmatrix}$ for a counter-clockwise BC Helix in a right-handed coordinate system:

$$\mathbf{V}(n) = \begin{bmatrix} r_{bc} \cos n\theta_{bc} \\ r_{bc} \sin n\theta_{bc} \\ nh_{bc} \end{bmatrix}, \quad (3)$$

where: $r_{bc} = \frac{3\sqrt{3}}{10} \approx 0.5196$,
 $h_{bc} = 1/\sqrt{10} \approx 0.3162$, and
 $\theta_{bc} = \arccos(-2/3)$,

and n represents each integer numbered vertex in succession on the z -axis.

The apparent rotation of a vertex on an outer-edge, that is $\mathbf{V}(n)$ relative from $\mathbf{V}(n+3)$ for any integer n in eq. (3), is $3\theta_{bc} - 2\pi$.

This formula defines a helix, but it is not any of the apparent helices, or *rail* helices, of the BC helix, but rather one that winds much more rapidly through all vertices. To a designer of tetrahelices, it is more natural to think of the three helices which are visually apparent, that is, those three which are closely approximated by the outer edges or rails of the BC helix. We think of each of these three rails as being a different color: red, blue, or yellow. This situation is illustrated in fig. 6, wherein the black helix represents that generated by eq. (3), and the colored helices are generated by eq. (4), below.

In order to develop the continuum of slightly irregular tetrahelices, we need a formula that gives us the vertices of just one rail helix, denoted by color c and integer vertex number n :

$$(\forall n \in \mathbb{Z}, \forall c \in \{0, 1, 2\} : \mathbf{H}_{BCcolored}(n, c) = \mathbf{V}(3n + c)).$$

Such a helix can be written:

$$\mathbf{H}_{BCcolored}(n, c) = \begin{bmatrix} r_{bc} \cos((3\theta_{bc} - 2\pi)n + c\theta_{bc}) \\ r_{bc} \sin((3\theta_{bc} - 2\pi)n + c\theta_{bc}) \\ 3h_{bc}(n + c/3) \end{bmatrix}, \quad (4)$$

where: $r_{bc} = \frac{3\sqrt{3}}{10}$,
 $h_{bc} = 1/\sqrt{10}$, and
 $\theta_{bc} = \arccos(-2/3)$.

In this formula, integral values of n may be taken as a vertex number for one rail and used to compute its Cartesian coordinates. Allowing n to take non-integer values defines

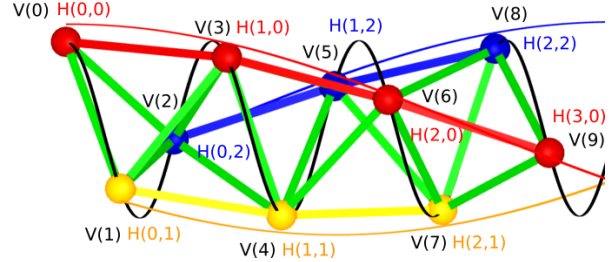


Fig. 6. Rail helices (H) vs. Coxeter/Gray helix (V)

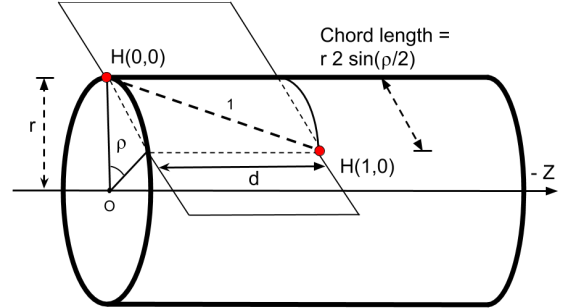


Fig. 7. Rail Angle Geometry

a continuous helix in space which is close to the segmented polyline of the outer tetrahedra edges, and equals them at integer values.

Figure 6 illustrates this difference with a 7-tetrahedra BC helix, which is in fact the same geometry as the robot illustrated in fig. 5. Although the vertices coincide, eq. (3) evaluated at real values generates the black helix which runs through every vertex, and eq. (4) defines the red, yellow, and blue helices. In this figure, these rail helices have been rendered at a slightly higher radius than the vertices for clarity; in actuality, the maximum distance between the continuous, curved helix and the straight edges between vertices is much smaller than can be clearly rendered.

The quantity $(3\theta_{bc} - 2\pi) \approx 35.43^\circ$ is the angular shift between adjacent vertices on the same rail: $\mathbf{V}(3n + c) = \mathbf{H}_{BCcolored}(n, c)$ and $\mathbf{V}(3(n+1) + c) = \mathbf{H}_{BCcolored}(n+1, c)$. This quantity appears so often that we call it the "rail angle, ρ ". For the BC helix, $\rho_{bc} = (3\theta_{bc} - 2\pi)$.

Note, in fig. 7, the z -axis travel for one rail edge is denoted by d . In eq. (3) and eq. (4), the variable h is used for one third of the distance, we name d . We will later justify that $d = 3h$. In this paper, we assume the length of a rail is always 1 as a simplification, except in proofs concerning rail length. We make the rail length a parameter in our JavaScript code in https://github.com/PubInv/tetrahelix/blob/master/js/tetrahelix_math.js [8].

The $\mathbf{H}_{BCcolored}(n, c)$ formulation can be further clarified by rewriting directly in terms of the rail angle ρ_{bc} rather than θ_{bc} . Intuitively, we seek an expression where $c/3$ is multi-

plied by a $1/3$ rotation plus the rail angle ρ . We expand the expressions θ_{bc} and ρ_{bc} in eq. (4) and seek to isolate the term $c2\pi/3$.

Thus, starting with the expression:

$$c\theta_{bc}$$

we introduce 3 into the denominator...

$$(c/3)(3\theta_{bc})$$

we want 2π in numerator, so add canceling terms...

$$(c/3)((3\theta_{bc} - 2\pi) + 2\pi)$$

...and then use the definition of ρ_{bc}

$$(c/3)\rho_{bc} + c2\pi/3$$

finally we obtain:

$$c(\rho_{bc} + 2\pi)/3. \quad (5)$$

This allows us to redefine:

$$\mathbf{H}_{BCcolored}(n, c) = \begin{bmatrix} r\cos\rho_{bc}n + c(\rho_{bc} + 2\pi)/3 \\ r\sin\rho_{bc}n + c(\rho_{bc} + 2\pi)/3 \\ (n + c/3)h_{bc} \end{bmatrix}, \quad (6)$$

where: $\rho_{bc} = (3\theta_{bc} - 2\pi)$, and
 $h_{bc} = 1/\sqrt{10}$.

Recall that $c \in \{0, 1, 2\}$, but n is continuous (rational or real-valued). We can now assert that in fig. 6 the black helix winds at $\frac{3\theta_{bc}}{\rho_{bc}} \approx 11.16$ times the rate of a rail helix.

From this formulation it is easy to see that moving one vertex on a rail ($\mathbf{H}_{BCcolored}(n, c)$) to $\mathbf{H}_{BCcolored}(n + 1, c)$ for any n and c) moves us ρ_{bc} radians around a circle. Since: $\frac{2\pi}{\rho_{bc}} \approx 10.16$ we can see that there are approximately 10.16 red, blue or yellow tetrahedra on one rail in a complete revolution of the tetrahelix.

The *pitch* of any tetrahelix, defined as the axial length of a complete revolution where $\rho \neq 0$ is:

$$p(\rho) = \frac{2\pi d}{\rho}. \quad (7)$$

The pitch of the Boerdijk-Coxeter helix of edge length 1 is the length of three tetrahedra times $p(\rho_{bc})$:

$$\frac{3h_{bc}2\pi}{\rho_{bc}} = \frac{6\pi}{\sqrt{10}\rho_{bc}} \approx 9.64. \quad (8)$$

The pitch is less than the number of tetrahedra because the tetrahedra edges are not parallel to the axis of the tetrahelix. It is a famous and interesting result that the pitch is irrational. A BC helix never has two tetrahedra at precisely the same orientation around the z -axis. However, this is inconvenient to designers, who might prefer a rational pitch. The idea of developing a rational period by arranging solid tetrahedra by relaxing the face-to-face matching has been explored [18]. We develop, below, slightly irregular edge lengths that support, for example, a pitch of precisely 12 tetrahedra in one revolution which would allow an architect to design a pleasing column having the top and bottom tetrahedra in the same relationship to the viewer on both the capital and the basis.

3 Optimal Tetrahelices are Triple Helices

We use the term *tetrahelix* to mean any structure physically constructible of vertices and finite edges which is isomorphic to the BC helix and in which the vertices lie on three helices. By isomorphic we mean there is a one-to-one mapping between both vertices and edges in the two tetrahelices. One could consider various definitions of optimality for a tetrahelix, but the most useful to us as roboticists working with the Tetrobot concept is to minimize the maximum ratio between any two edge lengths, because the Tetrobot uses mechanical linear actuators with limited range of extension.

A *triple helix* is three congruent helices that share an axis. We show that optimal tetrahelices are in fact triple helices with the same radius, so that all vertices are on a cylinder. In stages, we demonstrate that the helices in optimal tetrahelices:

1. have the same pitch,
2. have parallel axes,
3. share the same axis,
4. have the same radius,
5. have the same rail length,
6. have axially equidistant vertices, and therefore
7. are in fact triple helices.

Suppose that all three rails do not have the same pitch. If we start at any shortest edge between two rails, as we move from vertex to vertex away from our start edge, the edge lengths between rails must always lengthen without bound, which cannot be optimal. So we are justified in talking about the *pitch* of the optimal tetrahelix as the pitch of its three rail helices, even though there are three such helices of equivalent pitch.

Similarly, if the axes are not parallel, there is an edge of unbounded length in the structure, so we do not consider such cases.

Define a *minimax edge-length optimal tetrahelix* or just an *optimal tetrahelix* to be a tetrahelix for which there exists no other tetrahelix with lower ratio of longest edge length to shortest edge length.

We wish to show that in an optimal tetrahelix, all vertices lie on the cylinder of radius r , regardless of where they lie on the z -axis.

As a little lemma for the proof below, observe that a tetrahelix of zero radius, where all points lie on the same line, is not as optimal as a tetrahelix of a small radius. The edges between rails will be shorter than the rail edges, and moving them apart slightly lengthens the between-edge rails, improving the ratios.

In the proof, below, we find it useful to consider projection diagrams that are the axial projection of a tetrahelix onto the XY -plane. Figures 8 and 12 are examples of such a diagram.

Lemma 1. *If the rail angle $0 < \rho < \pi$ is a rational multiple of π , then the projection of edges in a helix of that rail angle along the z -axis onto the XY -plane form a regular polygon of 3 or more sides, or else they fill in a complete circle.*

Proof. All points lying on a helix projected along the axis lie on a circle in the XY -plane. Helices are periodic in the z -dimension modulo 2π . If $2\pi/\rho$ is irrational, the projection onto the XY -plane will contain an unbounded number of points on a circle. If and only if $2\pi/\rho$ is rational, the projection onto the XY -plane will contain a finite number of points. Because π is transcendental and irrational, $2\pi/\rho$ is rational if and only if $\rho = a\pi/b$, where a and b are integers and, without loss of generality, a and b are coprime. Since $\rho < \pi$, therefore $a < b$. Also, $\rho > 0$, therefore $a > 0$. The number of points in the projection is $2b$ if a is odd, and b if a is even. This polygon has at least 3 sides, since either ρ is irrational or $b > a$, and therefore $b \geq 2$. If $a/b = 1/2$, the projection is a square, which has four sides.

Theorem 1. *Any optimal tetrahelix with a rail angle of magnitude less than π has all three axes coincident.*

Proof. Case 1: Suppose that ρ is zero. Each helix has zero curvature, that is, it is a straight line. These lines are equivalent to some three degenerate helices with coincident axes, possibly with different radii, so long as there is a phase term in the definition of the helix, as in eq. (4). We later show the radii must be equivalent.

Case 2: Suppose that ρ is positive but less than π . In this case, each rail helix has curvature. The projection of points in the XY plane creates a figure guaranteed to have points on either side of any line through the axis of such a helix, because the figure is either an n -gon or a circle by lemma 1. We show that the three helices share a common axis.

Without loss of generality, define the Red helix to have its axis on the z -axis. Since there must be at least one Red-to-Yellow or a Red-to-Blue edge that is either a minimum or a maximum, without loss of generality, define the Blue helix to be a helix that has an edge connection to the Red helix that is either a maximum or a minimum. Let B' be a translation in the XY -plane of the blue helix B so that its axis is the z -axis and coincident with the red helix R . Let D be the distance between the axis of the Blue helix B and B' . We will show that if $D > 0$ then B “wobbles” in a way that cannot be optimal. Define a wobble vector by:

$$\mathbf{W}(n) = \mathbf{B}(n) - \mathbf{B}'(n). \quad (9)$$

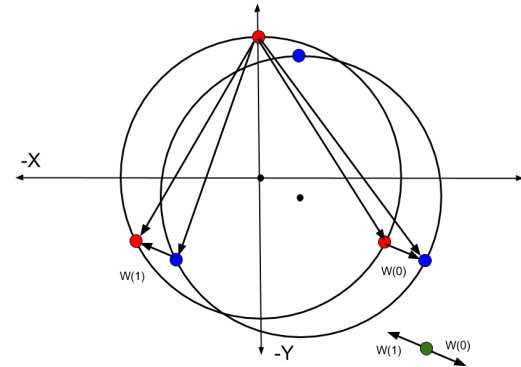


Fig. 8. Wobble Vectors from Non-Coincident Axes

where $\mathbf{B}(n)$ and $\mathbf{B}'(n)$ is the vector $\begin{bmatrix} x \\ y \end{bmatrix}$ for the projection of the n th vertex of B and B' . Note that $\|\mathbf{R}(n) - \mathbf{B}'(n+k)\|$ (the Euclidean distance of the vertices) is a constant for any k , because R and B' have the same pitch and the same axis, even if they do not have the same radius.

Figure 8 illustrates this situation. Like most diagrams, it is overspecific, in that the two circles are drawn of the same radius but we do not depend upon that in this proof. The diagram represents the projection along the z -axis of a few points into the XY -plane.

Since $\rho < \pi$ by assumption, by lemma 1, the set of wobblies $\{\mathbf{W}(n)|\text{for any } n\}$ contains at least three vectors, at least two of which point in different directions. For any point not at the origin, at least one of these vectors moves closer to the point and at least one moves further away.

The set of all lengths in the tetrahelix is a superset of: $L = \{\|\mathbf{R}(n) - \mathbf{B}(n)\|\}$, which, by our choice, has at least one longest or shortest length. $L = \{\|\mathbf{R}(n) - (\mathbf{B}'(n) + \mathbf{W}(n))\|\}$ and so $L = \{\|(\mathbf{R}(n) - \mathbf{B}'(n)) - \mathbf{W}(n)\|\}$. But $\mathbf{R}(n) - \mathbf{B}'(n)$ is a constant, so the minimax value of L is improved as $\|\mathbf{W}(n)\|$ decreases. By our choice that there is a Blue-to-Red edge that is either a maximum or a minimum, this improves the minimax value of the total tetrahelix.

This process can be carried out on both the Blue and Yellow helices (perhaps simultaneously) until $\mathbf{W}(n)$ is zero for both, finding a tetrahelix of improved overall minimax value at each step. So a tetrahelix is optimal only when $\mathbf{W}(n) = 0$, and therefore when $D = 0$ and $\mathbf{B}(n) = \mathbf{B}'(n)$, and all three axes are coincident.

Now that we have shown that axes are coincident and parallel and that the pitches are the same for all helices, we can assert that any optimum tetrahelix can be generated with an equation for helices:

$$\mathbf{V}_{\text{triple}}(n, c) = \begin{bmatrix} r_c \cos(n\alpha + c2\pi/3 + \phi_c) \\ r_c \sin(n\alpha + c2\pi/3 + \phi_c) \\ \frac{d(n+c/3)}{3} \end{bmatrix}, \quad (10)$$

where: $c \in \{0, 1, 2\}$, which would be much more

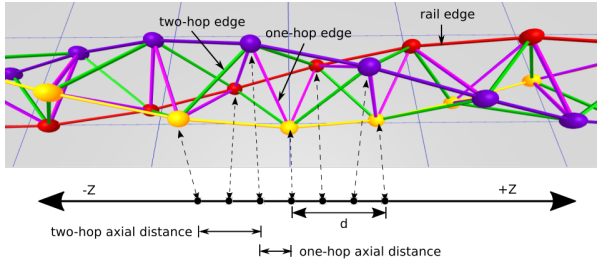


Fig. 9. Edge Naming

complicated if the axes where not coincident. Note that we have not yet shown that the relationships of the radius r_c or the phase ϕ_c for the three helices, so we denoted them with a c subscript to show they are dependent on the color. We have not yet investigated in the general case the relationships between α , r , ϕ and d in eq. (10). In section 4, we give a more specific version of this formula which generates optimal tetrahelices. We observe that when $\alpha = 0$, the helices are degenerate, having curvature of 0, but because of the ϕ_c term, they are not collinear.

In principle, any three helices generated with eq. (10) has at most nine distinct edge length classes. Each edge that connects two rails potentially has a longer length and shorter length we denote with a + or -. So the classes are $\{RR, BB, YY, RB_+, RB_-, BY_+, BY_-, RY_+, RY_-\}$. If when projecting all vertices onto the z -axis (dropping the x and y coordinates), the interval defined by the z -axis value of its endpoints contains no other vertices, we call it a *one-hop* edge, and if it does contain another vertex we call it a *two-hop* edge, as illustrated in fig. 9. Then there are 3 rail edges $\{RR, BB, YY\}$, 3 one-hop lengths $\{RB_-, BY_-, RY_-\}$ between each pair of 3 rails, and 3 two-hop lengths $\{RB_+, BY_+, RY_+\}$ between each pair of 3 rails, where the two-hop length is at least the one-hop length. However, if we symmetrically generate the three helices with eq. (10), many of these lengths will be the same. In fact, it is possible that there will be only two distinct such classes, and in fact in the purely regular BC helix there is only one length.

Theorem 2. *Optimal tetrahelices have the same radius for all three helices.*

Proof. To prove this theorem, we exhibit a symmetric tetrahelix (not yet shown to be optimal) which happens to be a triple helix, that has the property that all rail edges are equal to all one-hop edges and all two-hop edges are equal to each other. Observe that although we have not yet given the formula for the radii of such a triple helix, there are some values for r and α , and ϕ in eq. (10) for which all the three helices are symmetrically and evenly spaced. Furthermore, we can choose these values such that the three rail edges are of length 1 and so that the one-hop lengths are also all of length 1, and the two-hop lengths are slightly longer.

Now consider a tetrahelix in which the radius of one of the helices is different. By the connections made in a tetrahelix, any increase to a radius increases both a one-hop and two-hop distance, and any decrease likewise decreases two.

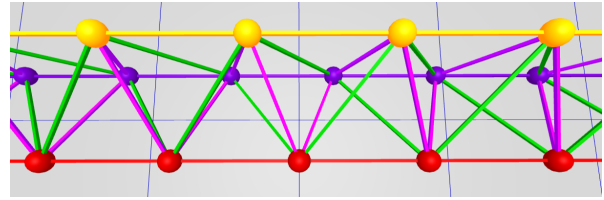


Fig. 10. Equitetrabeam

Since there exists a tetrahelix which has only two distinct classes of edge lengths, the smaller being one-hop = rail, the larger being the two-hop distance, the helix with a larger radius increases a longest edge without increasing a shortest edges. Likewise, a helix with a smaller radius decreases a one-hop edge without decreasing a two-hop edge. Therefore, a tetrahelix with different radii is not as optimal as some two-class tetrahelix generated by eq. (10), and so it is not optimal. We have not yet proved that a two-class tetrahelix is optimal, but it suffices to show that there exists such a better tetrahelix to show that different radii imply a suboptimal tetrahelix.

Because an optimal tetrahelix has equivalent radii and equivalent pitch for all three helices, it has equivalent rail edge lengths. Likewise, there is a single rail angle ρ that represents the rotation of two vertices connected by a single rail edge, and it is the same for all three rails.

Now that we have shown that on any optimal tetrahelix the vertices are on helices of the same axes and pitch, we see that the vertices of any optimal tetrahelix will lie on a cylinder, or a circle when the axis dimension is projected out. Therefore, it is reasonable to now speak of the singular radius r of a tetrahelix as the radius of the cylinder. We can now go on to the harder proof about where vertices occur along the z -axis.

We show that, in fact, the vertices must be distributed in even thirds along the z -axis as they are in the regular BC helix.

However, we have already shown the rail lengths are equal in any optimal tetrahelix.

Figure 10 shows the equitetrabeam, which is defined in section 6, but also conveniently illustrates the one-hop and two-hop edge definitions. The green edges are the two-hop edges and the purple edges are the one-hop edges. Note that the green edges are slightly longer than the purple edges. In fig. 9, which depicts the BC helix, the two-hop and one-hop edges are of equal length (but the projection onto the z -axis, the axial length, of the two-hop edge is longer than the axial one-hop length.)

Theorem 3. *An optimal tetrahelix of any rail angle $0 \leq \rho < \pi$ is a triple helix with all vertices evenly spaced at $d/3$ intervals on the z -axis. Any one tetrahedron in a tetrahelix has 1 rail edge, 2 one-hop edges connected to the rail, and 2 two-hop edges connected to the rail. The sixth edge is opposite of the rail edge and is a one-hop edge.*

Proof. Consider a tetrahelix in which the vertices are evenly spaced at $d/3$ intervals on the z -axis. Every edge is either

a rail edge, or it makes one hop, or two hops. All of the one-hop edges are equal length. All of the two-hop edges are equal length.

Every vertex is connected to 4 non-rail edges. There is a one-hop edge in both the positive and negative z direction. Likewise, there is a two-hop edge in both the positive and negative z direction. Let A be the set of edge lengths, which has only 3 members, represented by $A = \{o, t, r\}$ for the one-hop, two-hop, and rail edge lengths.

Any attempt to perturb any rail in either z direction lengthens one two-hop edge to t' , where $t' > t$ and shortens one one-hop edge $o' < o$. Let $B = \{o', t'\} \cup A$ be the edge lengths of such a perturbed tetrahelix. The minimax of B is greater than the minimax of A since there is a single rail length which cannot be both greater than o' and t' and less than o' and t' . Therefore, any optimal tetrahelix has all one-hop edges between all rails equal to each other, and all two-hop edges equal to each other, and the z distances between rails equal. Therefore, vertices are $d/3$ from each other on the z -axis.

Note that based on theorem 3, there are only 3 possible lengths in an optimal tetrahelix, and we are justified in classifying edge lengths as *rail*, *one-hop*, or *two-hop*. The one-hop edges are the edges between rails that are closest on the z -axis, and the two-hop edges are those that skip over a vertex.

Taking all of these results together, each helix in an optimal tetrahelix is congruent to the others, shares an axis, is the same radius, and is evenly spaced axially with the others. An optimal tetrahelix is therefore a *triple helix*, of a radius we have not yet demonstrated.

4 Parameterizing Tetrahelices via Rail Angle

We seek a formula to generate optimal tetrahelices that accepts a parameter that allows us to design the tetrahelix conveniently. Please refer back to fig. 7. The pitch of the helix is an obvious choice, but is not defined when the curvature is 0, an important special case. The radius or the axial distance between two vertices on the same rail are possible choices, but perhaps the clearest choice is to build formulae that takes as their input the “rail angle” ρ . We define ρ to be the angle formed in the X,Y plane with origin O : $\angle \mathbf{H}(0,0)O\mathbf{H}(0,1)$ projecting out the z -axis and sighting along the positive z -axis. In other words, ρ controls how far a rail edge of a tetrahelix deviates from being parallel with the axis, or the “twistiness” of the tetrahelix. We use the parameter $\chi = 1$ to indicate a chirality of counter-clockwise, and $\chi = -1$ for clockwise. We take our coordinate system to be right-handed.

The quantities ρ, r, d (see fig. 7) are related by the expression:

$$1^2 = d^2 + (2r \sin \rho/2)^2, \text{ or} \\ d^2 = 1 - 4r^2(\sin \rho/2)^2. \quad (11)$$

Checking the important special case of the BC helix, we find that this equation indeed holds true, treating d in this equation as $3h_{bc}$ as defined by Gray and Coxeter, that is, $d_{bc} = 3h_{bc}$, where they are using h for the axial height from one vertex to the next of a different color, but we use d to mean the axial distance between vertices of the same color.

The rail angle ρ also has the meaning that $2\pi/\rho$ is the number of tetrahedra in a full revolution of the helix.

In choosing ρ , one greatly constrains r and d , but does not completely determine both of them together, so we treat both as additional parameters.

Rewriting our formulation in terms of ρ :

$$\mathbf{H}_{\text{general}}(\chi, n, c, \rho, d_\rho, r_\rho) = \\ \begin{bmatrix} r_\rho \cos(\chi \cdot (n\rho + c(\rho + 2\pi)/3)) \\ r_\rho \sin(\chi \cdot (n\rho + c(\rho + 2\pi)/3)) \\ d_\rho(n + c/3) \end{bmatrix} \quad (12)$$

where: $1 = d_\rho^2 + 4r_\rho^2(\sin \rho/2)^2$, and
 $\chi \in \{-1, 1\}$.

$\mathbf{H}_{\text{general}}$ forces the user to select three values satisfying eq. (11): ρ , r_ρ , and d_ρ .

Note that when $\rho = 0$ then $d_\rho = 1$, but r_ρ is not determined by eq. (11).

Theorem 4. For rail angles of magnitude at most ρ_{bc} , tetrahelices generated by $\mathbf{H}_{\text{general}}$ are optimal in terms of minimum maximum (minimax) ratio of member length when radius is chosen so that the length of the one-hop edge is equal to the rail length.

Proof. By theorem 3, we can compute the (at most) three edge-lengths of an optimal tetrahelix by formulae universally quantified by n and c :

$$1 = \text{rail} = ||\mathbf{H}_{\text{general}}(n, c, \rho, d_\rho, r) - \\ \mathbf{H}_{\text{general}}(n+1, c, \rho, d_\rho, r)||, \quad (13)$$

$$\text{one-hop} = ||\mathbf{H}_{\text{general}}(n, c, \rho, d_\rho, r) - \\ \mathbf{H}_{\text{general}}(n, c+1, \rho, d_\rho, r)|| \text{ and}, \quad (14)$$

$$\text{two-hop} = ||\mathbf{H}_{\text{general}}(n, c, \rho, d_\rho, r) - \\ \mathbf{H}_{\text{general}}(n, c+2, \rho, d_\rho, r)||. \quad (15)$$

This syntax just represents the Euclidean distance between vertices. Thus:

$$\text{one-hop} = \sqrt{\frac{d_p^2}{9} + r^2(\sin^2(\rho/3 + \frac{2\pi}{3}) + (1 - \cos(\rho/3 + \frac{2\pi}{3}))^2)} \quad (16)$$

where: $d_p^2 = 1 - 4r^2(\sin(\rho/2))^2$.

By similar algebra and trigonometry:

$$\text{two-hop} = \sqrt{\frac{4d_p^2}{9} + r^2(\sin^2(2\rho/3 + \frac{4\pi}{3}) + (1 - \cos(2\rho/3 + \frac{4\pi}{3}))^2)}. \quad (17)$$

By definition of minimax edge length optimality, we are trying to minimize:

$$\frac{\max\{1, \text{one-hop}(r), \text{two-hop}(r)\}}{\min\{1, \text{one-hop}(r), \text{two-hop}(r)\}}.$$

But since $\text{two-hop}(r) \geq \text{one-hop}(r)$, this is equivalent to:

$$\frac{\max\{1, \text{two-hop}(r)\}}{\min\{1, \text{one-hop}(r)\}}.$$

This quantity will be equal to one of:

$$\frac{\text{two-hop}(r)}{1}, \frac{1}{\text{one-hop}(r)}, \frac{\text{two-hop}(r)}{\text{one-hop}(r)}. \quad (18)$$

We know that both $\text{one-hop}(r)$ and $\text{two-hop}(r)$ increase monotonically and continuously with increasing r . By inspection, it seems likely that we will minimize this set by equating $\text{one-hop}(r)$ or $\text{two-hop}(r)$ to 1, but to be absolutely sure and to decide which one, we must examine the partial derivative of the ratio $\frac{\text{two-hop}(r)}{\text{one-hop}(r)}$ in this range.

Although complicated, we can use Mathematica to investigate the partial derivative of $\frac{\text{two-hop}(r)}{\text{one-hop}(r)}$ with respect to the radius to be able to understand how to choose the radius to form the minimax optimum.

Let:

$$f_\rho = -\frac{4(\sin^2(\rho/2))}{9}, \quad (19)$$

$$g_\rho = -\frac{16(\sin^2(\rho/2))}{9}, \quad (20)$$

$$j_\rho = \sin^2(\rho/3 + \frac{2\pi}{3}) + (1 - \cos(\rho/3 + \frac{2\pi}{3}))^2, \quad (21)$$

and:

$$k_\rho = \sin^2(2\rho/3 + \frac{4\pi}{3}) + (1 - \cos(2\rho/3 + \frac{4\pi}{3}))^2. \quad (22)$$

Then:

$$\frac{\text{two-hop}(r)}{\text{one-hop}(r)} = \frac{\sqrt{\frac{4}{9} + r^2(g_\rho + j_\rho)}}{\sqrt{\frac{1}{9} + r^2(f_\rho + k_\rho)}}. \quad (23)$$

By graph inspection using Mathematica (<https://github.com/PubInv/tetrahelix/blob/master/tetrahelix.nb>), we see the partial derivative of this with respect to radius r is always negative, for any $\rho \leq \rho_{bc}$. When the rail angle approaches π , corresponding to going almost to the other side of the tetrahelix, this is not necessarily true, hence the limitation in our statement of the theorem is meaningful. Since the partial derivative of $\frac{\text{two-hop}(r)}{\text{one-hop}(r)}$ with respect to the radius r is negative for all ρ up until ρ_{bc} , this ratio goes down as the radius goes up, and we minimize the maximum edge-length ratio by choosing the largest radius up until $\text{one-hop} = 1$, the rail-edge length. If we attempted to further increase the radius we would not be optimal, because the ratio $\frac{\text{two-hop}(r)}{1}$ would become the largest ratio in our set of ratios eq. (18).

Therefore, we decrease the minimax length of the whole system as we increase the radius up to the point that the shorter, one-hop distance is equal to the rail-length, 1. In order to optimize the whole system so long as $\rho \leq \rho_{bc}$, we equate one-hop to 1 to find the optimum radius:

$$1 = \sqrt{\frac{\frac{1}{9}}{\sin^2(\rho/3 + \frac{2\pi}{3})} + \frac{r_{opt}^2(-\frac{4(\sin^2(\rho/2))}{9})}{(1 - \cos(\rho/3 + \frac{2\pi}{3}))^2}} \quad (24)$$

from which it follows that:

$$r_{opt} = \frac{2}{\sqrt{\frac{9}{2} \cdot (\sqrt{3}\sin(\rho/3) + \cos(\rho/3)) + \cos(\rho) + 8}}. \quad (25)$$

We can now give a formula for d_{opt} computed from ρ, r_{opt} via the rail angle equation eq. (11):

$$d_{opt}^2 = 1 - 4(r_{opt})^2(\sin\rho/2)^2, \quad (26)$$

which we can expand,

$$d_{opt}^2 = 1 - \frac{16(\sin\rho/2)^2}{9(\sqrt{3}\sin(\rho/3) + \cos(\rho/3)) + \cos(\rho) + 8} \quad (27)$$

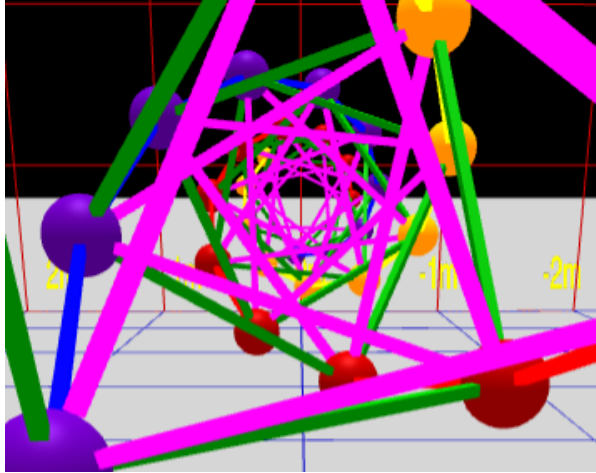


Fig. 11. Axial view of a BC-Helix

and then rewrite:

$$d_{opt} = \sqrt{1 - \frac{16 \sin^2(\rho/2)}{\cos(\rho) + 9(\sqrt{3} \sin(\rho/3) + \cos(\rho/3)) + 8}}. \quad (28)$$

Thus, by computing r_{opt} and d_{opt} as a function of ρ from this equation, we can construct a minimax optimal tetrahelix where $0 \leq \rho \leq \rho_{bc}$.

5 The Inradius

Since the axes are parallel, we may define the *inradius*, represented by the letter i , of a tetrahelix to be the radius of the largest cylinder parallel to this axis that is surrounded by each tetrahelix and penetrated by no edge.

If we look down the axis of an optimal tetrahelix as shown in fig. 11, it happens that only the one-hop edges (rendered in purple in our software) comes closest to the axis. In other words, they define the radius of the incircle of the projection, or the radius of a cylinder that would just fit inside the tetrahelix. A formula for the inradius of the tetrahelix is useful if you are designing it as a structure that bears something internally, such as a firehose, a pipe, or a ladder for a human. The inradius $r_{in}(\rho)$ of an optimal tetrahelix is a remarkably simple function of the radius r and the rail angle ρ :

$$r_{in}(\rho) = r \sin \frac{\pi - \rho}{6}, \quad (29)$$

which can be seen from the trigonometry of a diagram of the projected one-hop edges connecting four sequentially numbered vertices, shown in fig. 12.

From this equation, with the help of symbolic computation, we observe that inradius of the BC helix of unit rail length is $r_{in}(\rho_{bc}) = \frac{3}{10\sqrt{2}} \approx 0.21$.

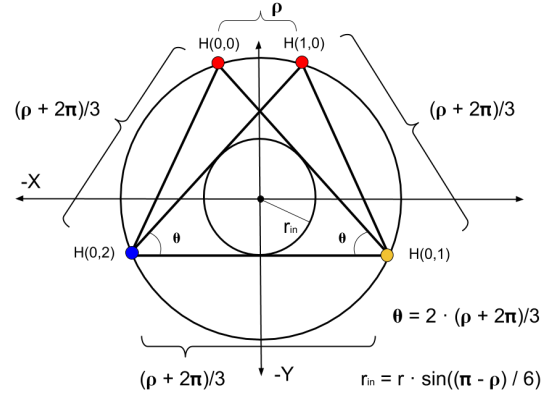


Fig. 12. General One-hop Projection Diagram

6 The Equitetrabeam

Just as $\mathbf{H}_{general}$ constructs the BC helix (with careful and non-obvious choices of parameters) which is an important special case due to its regularity, it constructs an additional special (degenerate) case when the rail angle $\rho = 0$ and $d = 1$ (the edge-length), where the cross sectional area is an equilateral triangle of unchanging orientation, as shown in fig. 10 and at the rear of fig. 3. We call this the *equitetrabeam*. It is not possible to generate an equitetrabeam from eq. (3) without the split into three rails introduced by eq. (4) and completed in eq. (12).

Corollary 1. *The equitetrabeam with minimum maximum edge ratio is produced*

by $\mathbf{H}_{general}$ when $r = \sqrt{\frac{8}{27}}$ and the longest member is $\frac{2}{\sqrt{3}}$, which is less than 16% longer than the shortest member.

Proof. Choosing $d = 1$ and $\rho = 0$ we use eq. (25) to find the radius of optimal minimax difference. Substituting into eq. (12) and setting one-hop¹ to 1 gives: $1 = \sqrt{\frac{1}{9} + 3r^2}$, or $r = \sqrt{\frac{8}{27}}$. This radius produces a two-hop edge length of $\frac{2}{\sqrt{3}} \approx 1.1547$.

The inradius of the equitetrabeam of unit rail length from both eq. (29) and the fact that the inradius of an equilateral triangle is half the circumradius is $\sqrt{\frac{8}{27}}/2$, or $\frac{\sqrt{6}}{9}$.

In fig. 3, the furthest tetrahelix is the optimal equitetrabeam. Figure 10 is a closeup of an equitetrabeam.

To the extent that we value tetrabeams (that is, tetrahelices with a rail angle of 0, and therefore zero curvature) as mathematical or engineering objects, we have motivated the development of $\mathbf{H}_{general}$ as a transformation of $\mathbf{V}(n)$ defined by eq. (3) from Gray and Coxeter.

The equitetrabeam may possibly be a novel construction. The fact that 6 members meet in a single point would

¹Before developing the optimal solution eq. (25) we found another interesting but non-optimal tetrabeam of zero curvature by setting the mean of one-hop and two-hop to 1 ((one-hop + two-hop)/2 = 1), which gives $r = \sqrt{35}/4$ and three length classes of $\frac{11}{12}, \frac{12}{12}, \frac{13}{12}$.

have been a manufacturing disadvantage that may have dissuaded structural engineers from using this geometry. However, the advent of additive manufacturing, such as 3D printing, and the invention of two distinct concentric multi-member joints [4, 5] has improved that situation.

Note that the equitetrabeam has chirality, which becomes important in our attempt to build a continuum of tetrahelices.

7 An Untwisted Continuum

We observe that eqs. (25) and (28) compute r_{opt} and d_{opt} which create an optimal tetrahelix for any rail angle ρ between 0, which gives the equitetrabeam and $\rho_{bc} \approx 35.43^\circ$, which gives the BC helix.

Because the equitetrabeam which has a rail angle of 0 still has chirality, that is, one still must decide to connect the one-hop edge to the clockwise or the counter-clockwise vertex, it is not possible to build a smooth continuum where ρ transitions from positive to negative which remains optimal. One can use a negative ρ in $\mathbf{H}_{general}$ but it does not produce minimax optimal tetrahelices. In other words, untwisting a counter-clockwise tetrahelix to rail angle 0 and then going even further does produce a clockwise tetrahelix, but one in which the one-hop and two-hop lengths in the wrong places, that is, two-hop becomes shorter than one-hop. Likewise, $\rho > \rho_{bc}$ generates a tetrahelix, but we have not proved or investigated optimality in that range.

The pitch of a helix for a known z -axis travel d is trivial (see eq. (7)). If one is varying ρ to obtain a desired pitch from eq. (28) and eq. (7) it is not so simple. However, the pitch increases monotonically and smoothly with decreasing ρ , so eq. (7) can be easily solved numerically with a Newton-Raphson solver, as we do on our website. For a pitch at least $p \geq \frac{3\sqrt{2}\pi}{\sqrt{5}\rho_{bc}} \approx 9.64$, using eq. (28) produces minimax optimal tetrahelices.

In this way, a rail angle can be chosen for any desired (sufficiently large) pitch, yielding the optimum radius, the one-hop length, and the two-hop length that an engineer needs to construct a physical structure.

The curvature of a rail helix is formally given by:

$$\frac{|r_\rho|}{r_\rho^2 + (d_\rho/\rho)^2}. \quad (30)$$

which goes to 0 as ρ approaches 0 (the equitetrabeam.) As ρ increase up to ρ_{bc} the curvature increases smoothly until the BC Helix is reached.

Perhaps surprisingly, the optimal untwisting is accomplished only by changing the length of the two-hop member, leaving the one-hop member and rail length equivalent within this continuum.² However, it should be noted that an engineer or architect may also use $\mathbf{H}_{general}$ directly

²Before deriving eq. (25), we created a continuum by using a linear interpolation between the optimal radius for the equitetrabeam and the BC Helix. This minimax optimum of this simpler approach was at most 1% worse than the optimum computed by eq. (25).

and interactively via <https://pubinv.github.io/tetrahelix/>, and that minimax length optimality is a mathematical starting point rather than the final word on the beauty and utility of physical structures. For example, a structural engineer might increase a radius past optimality in order to resist buckling.

If an equitetrabeam were actually used as a beam, an engineer might start with the optimal tetrabeam and dilate it in one dimension to stiffen the beam by deepening it. Similarly, simple length changes curve the equitetrabeam into an arch. The “colored” approach of eq. (12) exposes these possibilities more than the approach of eq. (3).

8 Conclusion

It is proven there exists a continuum of minimax edge-length optimal tetrahelices having as one end the completely regular Boerdijk-Coxeter Helix and at the other end a completely untwisted tetrahelix with equilateral cross section and planar faces, the equitetrabeam. By changing the length of only one out of three members by less than 16%, all configurations in the continuum may be reached. All such optimal tetrahelices may provably be generated by a simple equation giving coordinates or by selecting appropriate edge lengths generated from the same equation. A machine, such as a robot or a variable-geometry truss, that can change the length of some of its members by 16% can thus twist and untwist itself. A completely regular Tetrobot can untwist itself to create a planar face on the ground for locomotion. With a numeric solution, a designer may choose a rotation angle to obtain an optimal tetrahelix design of any pitch, including rational ones.

9 Contact and Getting Involved

The Tetrobot Project:

<http://pubinv.github.io/tetrobot/> is part of Public Invention, a free-libre, open-source research, hardware, and software project that welcomes volunteers. To assist, contact: read.robert@gmail.com.

References

- [1] Coxeter, H., et al., 1985. “The simplicial helix and the equation $\tan(n \theta) = n \tan(\theta)$ ”. *Canad. Math. Bull.*, **28**(4), pp. 385–393.
- [2] Read, R. L., 2016. Gluss = Slug + Truss. Unpublished preprint.
- [3] Hamlin, G. J., and Sanderson, A. C., 2013. *Tetrobot: A Modular Approach to Reconfigurable Parallel Robotics*. Springer Science & Business Media.
- [4] Song, S., Kwon, D., and Kim, W., 2003. Spherical joint for coupling three or more links together at one point, May 27. US Patent 6,568,871.
- [5] Hamlin, G. J., and Sanderson, A. C., 1994. “A novel concentric multilink spherical joint with parallel robotics applications”. In Proceedings of the 1994

- IEEE International Conference on Robotics and Automation, pp. 1267–1272 vol.2.
- [6] Fuller, R., 1961. Synergetic building construction, May 30. US Patent 2,986,241.
 - [7] Fuller, R., and Applewhite, E., 1982. *Synergetics: explorations in the geometry of thinking*. Macmillan.
 - [8] Read, R. L., 2017. Untwisting the tetrahelix website. <https://pubinv.github.io/tetrahelix/>.
 - [9] Mikulas, M., and Crawford, R., 1985. Sequentially deployable maneuverable tetrahedral beam, Dec. 10. US Patent 4,557,097.
 - [10] Claypool, J., 2012. Readily configured and reconfigured structural trusses based on tetrahedrons as modules, Sept. 18. US Patent 8,266,864.
 - [11] Gezgin, A. G., and Korkmaz, K., 2017. “A new approach to the generation of retractable plate structures based on one-uniform tessellations”. *Journal of Mechanisms and Robotics*, **9**(4), p. 041015.
 - [12] Sanderson, A. C., 1996. “Modular robotics: Design and examples”. In Emerging Technologies and Factory Automation, 1996. EFTA’96. Proceedings., 1996 IEEE Conference on, Vol. 2, IEEE, pp. 460–466.
 - [13] Lee, W. H., and Sanderson, A. C., 2002. “Dynamic rolling locomotion and control of modular robots”. *IEEE Transactions on robotics and automation*, **18**(1), pp. 32–41.
 - [14] NTRT, 2016. NTRT - NASA Tensegrity Robotics Toolkit. <https://ti.arc.nasa.gov/tech/asr/intelligent-robotics/tensegrity/ntrt/>. Accessed: 2016-09-13.
 - [15] Chen, L.-H., Kim, K., Tang, E., Li, K., House, R., Zhu, E. L., Fountain, K., Agogino, A. M., Agogino, A., SunSpiral, V., et al., 2017. “Soft spherical tensegrity robot design using rod-centered actuation and control”. *Journal of Mechanisms and Robotics*, **9**(2), p. 025001.
 - [16] Mirletz, B. T., Park, I.-W., Flemons, T. E., Agogino, A. K., Quinn, R. D., and SunSpiral, V., 2014. “Design and control of modular spine-like tensgrity structures”. In World Conference of the International Association for Structural Control and Monitoring (IACSM), IACSM.
 - [17] Gray, R. W., 2017. Tetrahelix data. <http://www.rwgrayprojects.com/rbfnotes/helix/helix01.html>.
 - [18] Sadler, G., Fang, F., Kovacs, J., and Irwin, K., 2013. “Periodic modification of the Boerdijk-Coxeter helix (tetrahelix)”. *arXiv preprint arXiv:1302.1174*.